Journal Pre-proofs

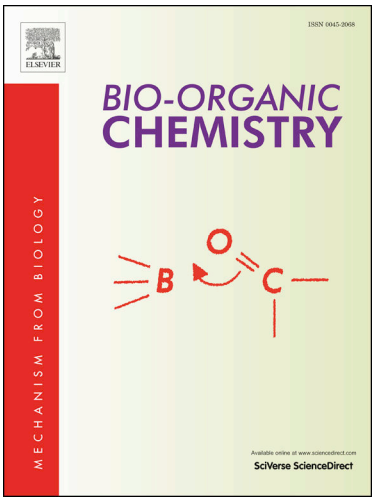

Synthesis, *in vitro*, and *in vivo* (Zebra fish) antitubercular activity of 7,8-dihydroquinolin-5(6*H*)-ylidenehydrazinecarbothioamides

Sandeep kumar Marvadi, Vagolu Siva Krishna, Goverdhan Surineni, Rudraraju Srilakshmi Reshma, Balasubramanian Sridhar, Dharmarajan Sriram, Srinivas Kantevari

PII: S0045-2068(19)31149-6
DOI: https://doi.org/10.1016/j.bioorg.2020.103626
Reference: YBIOO 103626

To appear in: *Bioorganic Chemistry*

Received Date: 20 July 2019
Revised Date: 28 December 2019
Accepted Date: 23 January 2020

Please cite this article as: S. kumar Marvadi, V. Siva Krishna, G. Surineni, R. Srilakshmi Reshma, B. Sridhar, D. Sriram, S. Kantevari, Synthesis, *in vitro*, and *in vivo* (Zebra fish) antitubercular activity of 7,8-dihydroquinolin-5(6*H*)-ylidenehydrazinecarbothioamides, *Bioorganic Chemistry* (2020), doi: https://doi.org/10.1016/j.bioorg.2020.103626

Synthesis, *in vitro*, and *in vivo* (Zebra fish) antitubercular activity of 7,8-dihydroquinolin-5(6*H*)-ylidenehydrazinecarbothioamides

Sandeep kumar Marvadi,[a] Vagolu Siva Krishna,[b] Goverdhan Surineni,[a] Rudraraju Srilakshmi Reshma,[b] Balasubramanian Sridhar,[c,d] Dharmarajan Sriram,[b] Srinivas Kantevari,[*a,d]

[a] *Fluoro and Agrochemicals Division, CSIR- Indian Institute of Chemical Technology, Hyderabad-500007, Telangana, INDIA.*

[b]*Medicinal Chemistry and Antimycobacterial Research Laboratory, Pharmacy Group, Birla Institute of Technology and Science-Pilani, Hyderabad Campus, Jawahar Nagar, Hyderabad-500078, Telangana, India.*

[c] *Division of X-ray Crystallography, CSIR-Indian Institute of Chemical Technology, Uppal Road, Hyderabad 500007, India.*

[d]*Academy of Scientific and innovative Research, CSIR- Indian Institute of Chemical Technology, Hyderabad-500 007, Telangana, India.*

Abstract:

We, herein, describe the synthesis of a series of novel aryl tethered 7,8-dihydroquinolin-5(6*H*)-ylidenehydrazinecarbothioamides **4a–v**, which showed *in vitro* and *in vivo* antimycobacterial activity against *Mycobacterium tuberculosis (Mtb)* H37Rv. The intermediates dihydro-6*H*-quinolin-5-ones **3a-v** were synthesized from β-enaminones, reacting with cyclochexane-1,3-dione/5,5-dimethylcyclohexane-1,3-dione and ammonium acetate using a modified Bohlmann-Rahtz reaction conditions. They were further reacted with thiosemicarbazide to give the respective hydrazine carbothioamides **4a-v**. All the new analogues **4a–v**, were characterized by their NMR and mass spectral data analysis. Among the twenty-two compounds screened for *in vitro* antimycobacterial activity against *Mycobacterium tuberculosis* H37Rv (ATCC27294), two compounds, **4e** and **4j**, exhibited the highest inhibition with an MIC of 0.39µg/mL. Compounds **4a, 4g**, and **4k** were found to inhibit *Mtb* at an MIC of 0.78µg/mL. Hydrazinecarbothioamides **4a-k**, exhibited enhanced activity than dihydroquinolinones **3a-k**. The observed increase in potency provides a clear evidence that hydrazinecarbothioamide is a potential pharmacophore, collectively imparting synergistic effect in enhancing antitubercular activity of the dihydroquinolinone core. The *in vivo* (Zebra fish) antimycobacterial screening of the *in vitro* active molecules led to the identification of a hit compound, **4j**, with significant activity in the *Mtb* nutrient starvation model (2.2-fold reduction). Docking studies of **4j** showed a hydrogen bond with the P156 residue of the protein.

Keywords:

Dihydroquinoline; hydrazinecarbothioamides; Mycobacterium tuberculosis; Nutrient Starvation; Zebra fish; Molecular docking.

1. Introduction

Tuberculosis (TB) is considered to be an inordinately spreading contagious disease, which arises due to *Mycobacterium tuberculosis* (*Mtb*) infection, and claims life of more people than malaria or HIV/AIDS [1]. As per the global TB report released by the World Health Organization (WHO), around 1.5 million people died and 11 million new TB cases were registered [2-7]. Further, the rapid emergence of multi-drug resistant (MDR) and extremely drug resistant (XDR) and totally drug resistant TB (TDR) tuberculosis cases are of major concern. It is evident from the literature/clinical data that the existing pool of drugs such as isoniazid (INH), rifampicin (RIF), and fluoroquinolones are becoming less sensitive (**Figure 1**) [8-10]. The new generation quinoline based drug Bedaquiline, approved by FDA for medical use in 2012, suffers from cardiovascular adverse effects [11,12]. Another drug Delamanid, a mycolic acid biosynthesis inhibitor has been approved for treating MDR-TB in South Korea, Europe and Japan [13].

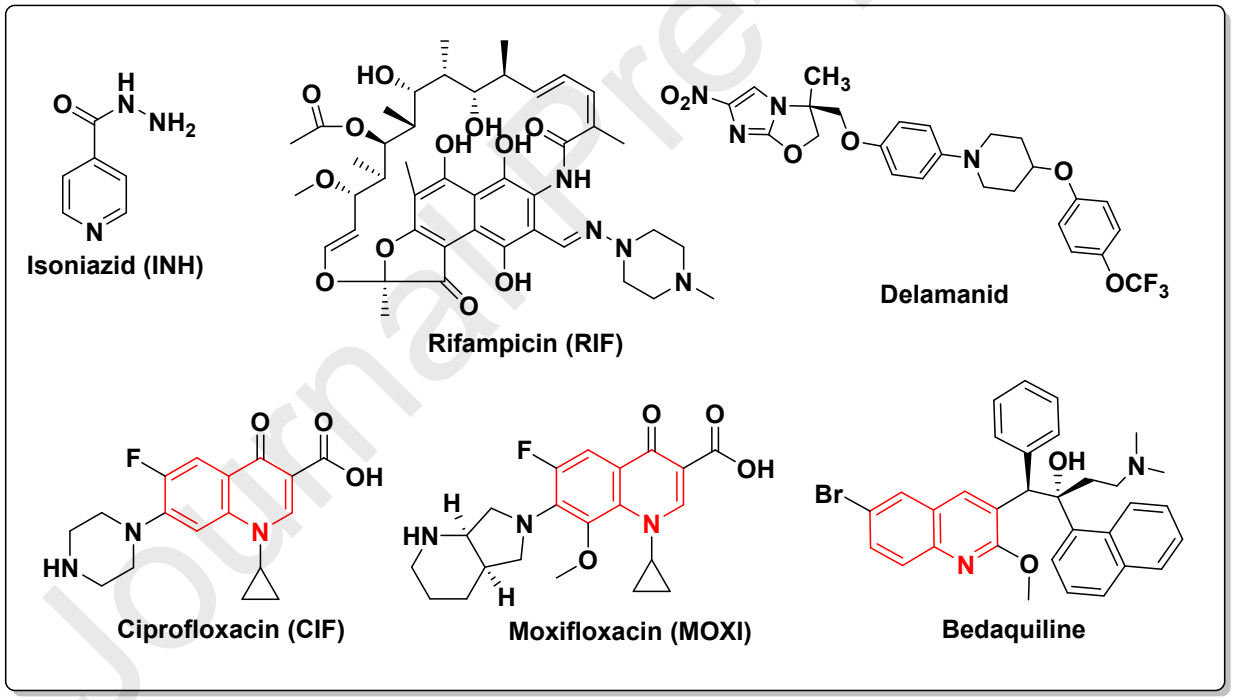

Figure 1. Representative anti-tubercular drugs.

In the recent years, molecules bearing thiosemicarbazones have been investigated extensively for their various pharmacological properties like antiviral, antifungal, antineoplastic,

antimycobacterial, and antimalarial effects. The versatility of sulphur and nitrogen atoms to act as donors allows them to bring in a great variety of coordination modes with bacterial protein. Many derivatives containing thiosemicarbazone moiety have been synthesized and evaluated for their antibacterial activity. Thiacetazone, (TAC; p-acetamidobenzaldehyde thiosemicarbazones also known as thioacetazone), is one of the oldest and cheapest second line drug used for tuberculosis treatment (**Figure 2**). But this drug shows only bacteriostatic activity, and develops resistance easily during tuberculosis therapy. It also has cross-resistance to ethionamide. Owing to its high frequency of Stevens-Johnson syndrome, thioacetazone is forbidden to use in patients with human immunodeficiency virus (HIV). To counter such affects, newer agents such as SRI-286 [14], SRI-224 and KBF-611 [15] bearing thiosemicarbazide are in clinical trials for treating tuberculosis (**Figure 2**). Although Thiacetazone (TAC) thought to inhibit mycolic acid biosynthesis, the exact mechanism of action has proven elusive. Recent studies of Jackson *et al* [16, 17] throw light on the mechanistic aspects of thioacetazone and other carbothiamide analogues and led to the speculation that there could be other enzymes playing role in the inhibition against *Mycobacterium tuberculosis*. As part of global efforts to develop an efficient antitubercular drug, our group is focused on the development of new dihydroquinolone based chemical entities as potential antitubercular agents. In view of the importance of the thiosemicarbazide moiety, we envisaged to hybridize dihydro-6*H*-quinolin-5-one with thiosemicarbazide pharmacophore. In the present paper, a series of novel 7,8-dihydroquinoline-5(6*H*)ylidene)hydrazinecarbothioamide derivatives, **4a-v**, were synthesized and evaluated for the *in vitro* inhibitory effect on pathogenic bacterium, *Mycobacterium tuberculosis* H37Rv. Among the 22 new derivatives, five compounds **4e, 4j** (MIC 0.39µg/mL), and **4a, 4g, 4k** (MIC 0.78µg/mL) resulted as the most promising antitubercular agents. The *in vivo (Zebra fish)* antimycobacterial screening of the active molecules led to the identification of an important hit compound **4j**, which may be pursued for further development.

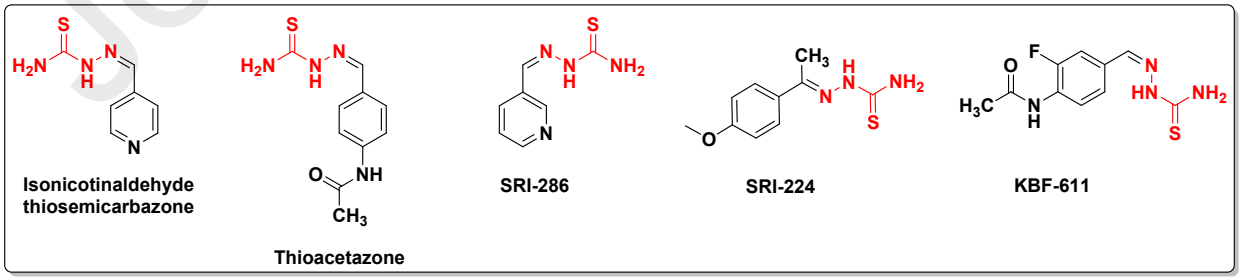

Figure 2. Thiosemicarbazide scaffold based antitubercular agents.

2. Results and discussion

2.1. Chemistry

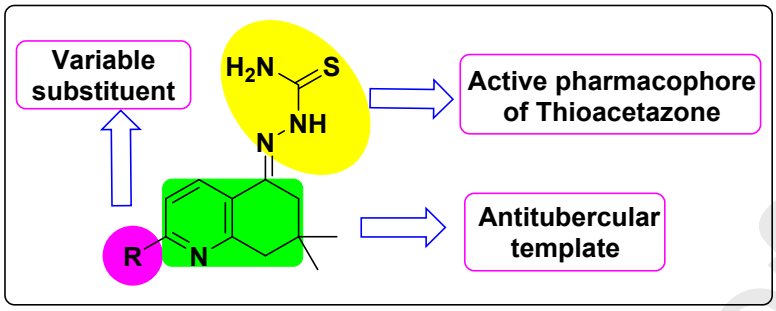

Figure 3. Molecular structure of hydrazinecarbothioamide derivatives used in the present study.

Broadly, the designed scaffold has three fragments. The first fragment is the dihydroquinoline pharmacophore from our previous reports, with antitubercular activity [18, 19]. The second fragment, hydrazinecarbothioamide, is a key pharmacophore present in antitubercular drugs such as thioacetazone. The third fragment is a variably substituted aryl and heteroaryl groups appended to dihydroquinoline moiety. Maneuvering all these three fragments into single molecular frame could impart or enhance antitubercular properties into the newer scaffold, 7,8-dihydroquinolin-5(6*H*)-ylidenehydrazine carbothioamides (**Figure 3**).

The target molecules, **4a-v**, were synthesized by following a three-step synthetic protocol described in Scheme 1. β-Enaminones, **2a-k**, were prepared by refluxing aryl and heteroaryl methyl ketones **1a-k**, with *N*,*N*-DMF-DMA in xylene. Compounds **2a-k** were reacted with cyclochexane-1,3-dione or 5,5-dimethyl-cyclohexane-1,3-dione, and NH_4OAc in the presence of $CeCl_3.7H_2O$-NaI in *i*-PrOH at reflux temperature to result the dihydro-6*H*-quinolin-5-ones **3a-v** in very good yields [18-28]. Compounds **3a-v** were condensed with thiosemicarbazide in methanol in the presence of catalytic amount of conc. H_2SO_4 to give desired 7,8-dihydroquinolin-5(6*H*)-ylidene)hydrazinecarbothioamide **4a-v** in excellent yields (**Table 1**). All the synthesized compounds were purified over a silica gel column and were fully characterized by IR, ^1H and ^{13}C NMR, electrospray ionization (ESI), and high-resolution mass spectral (HRMS) data analysis (Supporting Information). For example, ^1H NMR spectral data of compound **4j** showed aromatic protons at δ 10.13 - 7.00, the methylene (-CH_2) protons appeared at δ 2.90 (2H) as triplet (J = 6.0 Hz), δ 2.74 (2H) as triplet (J = 6.2 Hz), and δ 1.98 (2H) as

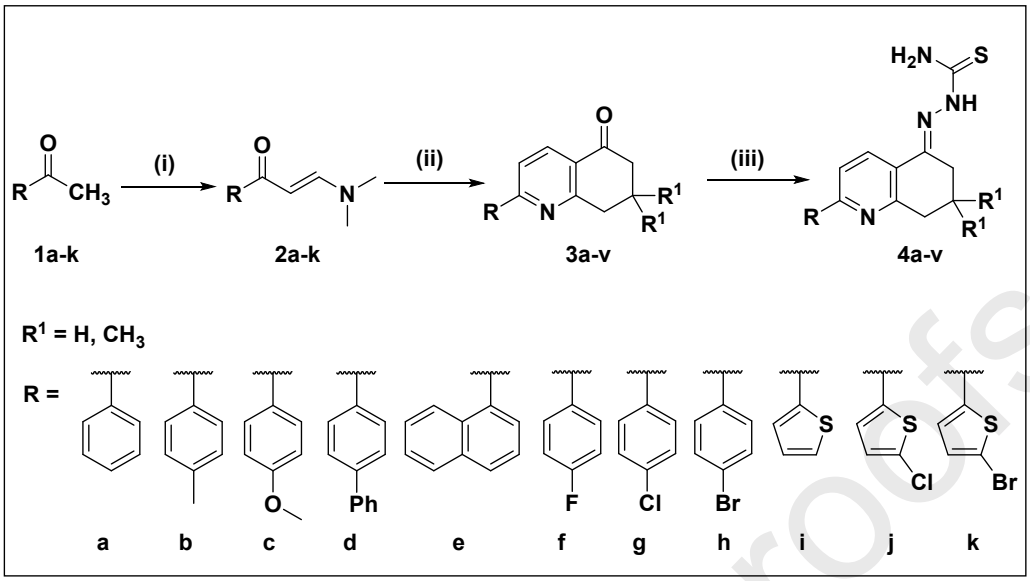

Scheme 1. Synthesis of compounds **4a–v**. *Reagents and conditions*: (i) *N*,*N*-DMF-DMA, xylene, reflux, 7 h, 95%; (ii) cyclohexane-1,3-dione/ 5,5-dimethyl cyclohexane-1,3-dione, NH_4OAc, $CeCl_3.7H_2O$-NaI, *i*-PrOH, reflux, 4 h, 86-94%; (iii) $NH_2CSNHNH_2$, conc. H_2SO_4, MeOH, reflux, 4 - 5 h, 76–92%.

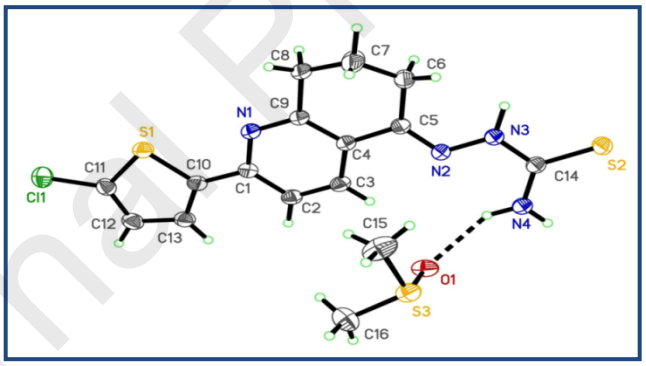

Figure 4. ORTEP representation of compound **4j** with the thermal displacement ellipsoids drawn at 30% probability. CCDC 1511250 contains supplementary crystallographic data for the structure.

quintet (J = 6.0 Hz), respectively. ^{13}C NMR spectrum showed methylene carbons at δ 31.6, 25.0, 20.3. HRMS data analysis of **4j** displayed a molecular ion peak at m/z 337.03429 $[M+H]^+$ suggesting the molecular formula as $C_{14}H_{14}N_4ClS_2$ of the said compound. Additionally, the IR spectra for the target compounds **4a-v** exhibited characteristic absorption bands at 3427-3137 cm^{-1}, 1588-1502 cm^{-1} and 1089-1026 cm^{-1} which corresponded to N-H (stretch), N-H (bend) and C=S respectively. The structure of compound **4j** was further confirmed by single crystal X-ray analysis **(Figure 4**).

2.2. Pharmacological evaluation

2.2.1. Antimycobacterial activity

All the synthesized 7,8-dihydroquinoline-5(6*H*)ylidene)hydrazinecarbothioamides, **4a-v**, were screened for their *in vitro* antimycobacterial activity against *M. tuberculosis* H37Rv (ATCC27294) strain by using the broth dilution method to determine the Minimum Inhibitory Concentration (MIC) [29,30]. The tested compounds exhibited an MIC range of 0.39µg/mL-25.0µg/mL (**Table 1**). Two compounds **4e** and **4j**, displayed potent antitubercular activity with an MIC of 0.39µg/mL. Compounds **4a, 4g**, and **4k** (MIC 0.78 µg/mL) also exhibited potent antitubercular effect on H37Rv. In addition to these five compounds, another five compounds **4b**, **4c**, **4f**, **4h**, and **4i (**MIC 1.56 µg/mL) exhibited greater inhibitory activity than standard drugs ethambutol and pyrazinamide. Two compounds **4d** and **4s** (MIC 3.125 µg/mL) were found to be equipotent to the standard drug ethambutol. Among other derivatives, compound **4p** exhibited MIC 12.5 µg/mL, two compounds **4n**, and **4o** (MIC of 25 µg/mL), and **4l**, **4m**, **4q**, **4r**, and **4t-v** were not active at an MIC of 25 µg/mL (**Table 1**). Compounds **4a-k** inhibited *M. tuberculosis* at much lower concentrations (MIC 0.39-3.13 µg/mL) compared to the compounds **4l-v** (MIC 3.13- >25.0µg/mL) implying that unsubstituted 1,3-cyclohexanedione is more active than its dimethylated counterpart. Although most of the compounds **4a-k** significantly inhibited *Mtb*, the MIC is slightly varied with respect to the substituent on phenyl ring or thiophene ring coupled to quinoline core. The substituent on quinoline core with respect to potency is varied in the order- **4e** (naphthyl), **4j** (chlorothiophenyl) with an MIC value of 0.39µg/mL > **4a** (phenyl), **4g** (4-chlorophenyl), **4k** (bromothiophenyl) with an MIC value of 0.78µg/mL > **4b** (4-methylphenyl),

Table 1. Antituberculosis evaluation of 4a–v against *M.tuberculosis* H37Rv and cytotoxicity.

Entry	Product	R	R^1	Yield (%)[a]	MIC (µg/mL)		Cytotoxicity % Inhibition at 50 µg/mL
					4a-v	3a-v	
1	**4a**	a	H	92	0.78	12.5	41.02
2	**4b**	b	H	89	1.56	12.5	32.42
3	**4c**	c	H	86	1.56	12.5	28.08
4	**4d**	d	H	88	3.13	>25.0	42.78
5	**4e**	e	H	82	0.39	>25.0	20.36

6	**4f**	f	H	80	1.56	NT	24.64
7	**4g**	g	H	83	0.78	>25.0	37.15
8	**4h**	h	H	81	1.56	NT	34.28
9	**4i**	i	H	85	1.56	12.5	27.58
10	**4j**	j	H	86	0.39	6.25	18.24
11	**4k**	k	H	83	0.78	6.25	21.08
12	**4l**	a	CH_3	85	>25.0	>25.0	NT
13	**4m**	b	CH_3	76	>25.0	>25.0	NT
14	**4n**	c	CH_3	81	25.0	12.5	NT
15	**4o**	d	CH_3	79	25.0	>25.0	NT
16	**4p**	e	CH_3	84	12.5	1.56	36.94
17	**4q**	f	CH_3	82	>25.0	NT	NT
18	**4r**	g	CH_3	82	>25.0	12.5	NT
18	**4s**	h	CH_3	78	3.13	12.5	39.48
20	**4t**	i	CH_3	80	>25.0	6.25	NT
21	**4u**	j	CH_3	82	>25	3.13	NT
22	**4v**	k	CH_3	81	>25	3.13	NT
23	Isoniazid	---	---	---	0.1		NT
24	Rifampicin	---	---	---	0.2		NT
25	Ethambutol	---	---	---	3.13		NT
26	Pyrazinamide	---	---	---	50		NT

[a] Isolated yield; NT – not tested.

4c (4-methoxyphenyl), **4f** (4-fluorophenyl), **4h** (4-bromophenyl), and **4i** (thiophenyl) with an MIC value of 1.56μg/mL > **4d** (4-biphenyl) with an MIC value of 3.13 μg/mL. On the other hand, compounds **4l-v**, with *gem*-dimethyl group, irrespective of the aryl substituent, showed significant reduction in antitubercular potency. Compound **4s** (bromophenyl, MIC-3.13μg/mL) showed good activity among compounds **4l-v**. It was interesting to note that the panel of compounds **4a-k**, containing hydrazinecarbothioamide, exhibited enhanced activity by several folds than dihydroquinolinones **3a-k** without hydrazinecarbothioamide, even when the other frameworks and substituents are same (Entries 1-11, Table 1). This observed increase in potency provides clear evidence that hydrazinecarbothioamide, consisting a free thiourea moiety along with ionizable proton, is a potential pharmacophore, collectively imparting synergetic effect on enhancing antitubercular activity to dihydroquinolinone core. To our surprise, compounds **4l-v** with gem-dimethyl group (Entries 12-22, Table 1), and hydrazinecarbothioamide could not induce synergistic effect and in few cases (Entries 16, 21, and 22, Table 1) dihydro-6*H*-quinolin-5-ones

without hydrazinecarbothioamide were more potent. The overall structure activity relationship (SAR) of the synthesized compounds **4a-v** is presented in **Figure 5**.

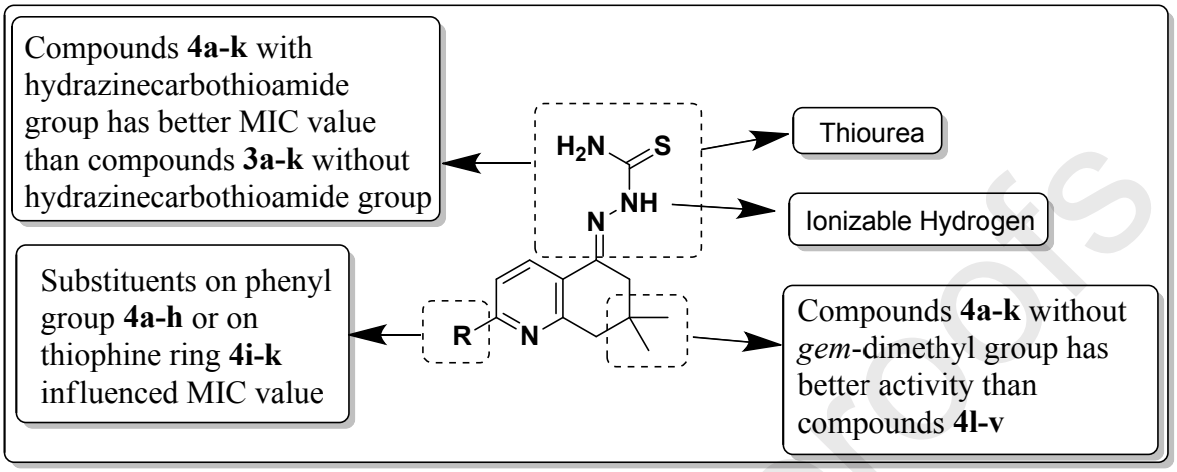

Figure 5: SAR of dihydroquinolin-5(6*H*)-ylidene)hydrazinecarbothioamide derivatives **4a–v.**

2.2.2. *In vitro* cytotoxicity

The active analogues from antitubercular assay (MIC ≤ 12.5 µg/mL) was assessed for *in vitro* cytotoxicity at 50µg/mL concentration against Human Embryonic Kidney (HEK-293T) cells using 3-(4,5-dimethylthiazol-2-yl)-2,5-diphenyltetrazolium bromide (MTT) assay [31, 32]. Percentage inhibition of cells is reported in **Table 1**. The most promising antitubercular compounds **4e**, **4j**, and **4a**, **4g**, **4k**, and **4b**, **4c**, **4f**, **4h**, **4i** exhibited 20.36%, 18.24%, and 41.02%, 37.15%, 21.08%, and 32.42%, 28.08%, 24.64%, 34.28%, 27.58% inhibition, respectively. The results clearly indicated that the most potent analogues **4e** and **4j** with high antitubercular activity are less toxic to Human Embryonic Kidney (HEK-293T) cells and are suitable for further mechanistic evaluations. The ratio between cytotoxicity and antimycobacterial activity in vitro enabled the determination of selectivity index (SI). Compounds that exhibited SI values greater than 10 in all four cell lines were considered nontoxic [20].

2.2.3. *Mycobacterium tuberculosis* H37Rv nutrient starved model.

The nutrient starvation model, developed by Betts et. al., has successfully been utilized by medicinal chemists to test compounds as antimycobacterial agents. The model mimics bacterial

characteristics in its persistent state causing bacterial growth arrest by nutrient starvation, minimizing aerobic metabolism while maintaining viability. We performed this assay with the most active compounds to identify the log reduction in the bacterial population and the results are show in **Figure 6**. Here, the dormancy in bacteria is induced by starving the culture in phosphate buffer saline (PBS) for 6 weeks. The dormant culture was tested with compounds **4e**, **4g**, **4j**, and **4k** at a concentration of 10 µM based on their MIC data [33,34]. Compounds **4e**, **4g**, **4j**, and **4k** showed a log reduction of 0.7, 2.1, 2.2, and 0.9, respectively. By comparison, standards INH and MOXI shown a log reduction of 1.5, and 2.0 respectively, compared to the control. The study reveals that the inhibition of dormant mycobacterium by new compounds can be beneficial towards the development of lead molecules to combat tuberculosis.

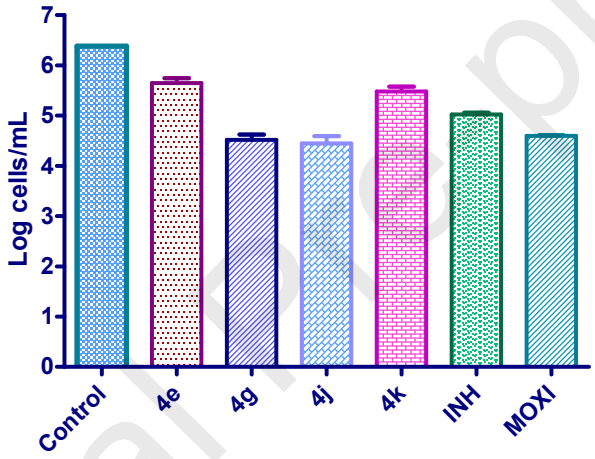

Figure 6. Activity profile of **4e, 4g, 4j and 4k** in nutrient starvation model. Bacterial count was estimated through MPN (most probable number) assay and significance plot was developed by adopting two-way ANOVA ($p < .0001$, using GraphPad Prism Software).

2.2.4. *In vivo* activity testing assay on *Mycobacterium marinum* infected zebra fish

Despite the extensive *in vitro* evaluation of *Mycobacterium tuberculosis* inhibitors, validation of the data in the animal models is essential. Of the several animal models developed for *Mycobacterium tuberculosis* infection, the most versatile one has been the mouse model. However, it has limitations like failure in caseating granulomas observed in humans. In this scenario, zebra fish infection model, using *M. marinum,* a genetic relative of *M. tuberculosis* is utilized complementary to the above models [35]. Activity and dosage of antibiotics in zebra fish is close

to that of the dosage in humans. This could be the most cost-effective and trustworthy model for researchers to study the *in vivo* activity of new drug compounds [35]. In this study, zebra fish was infected with *M. marinum* which genetically belongs to MTB family. Active molecule **4j** was tested for *in vivo* inhibitory activity using adult zebra fish model. Standard compounds INH and MOXI have shown reductions of 2.8 and 2.6 in log scale and compound **4j** has shown 2.3 log reductions against control (**Figure 7**).

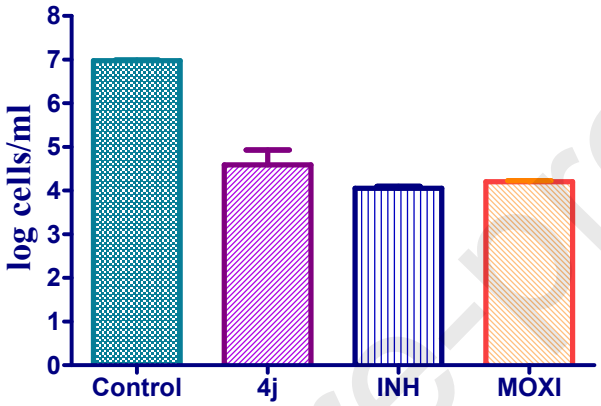

Figure 7. Bacterial count estimation (Mean ± S.E.M., n = 6) for control and treated groups by zebra fish model conducted by using MPN assay. Statistical significance has been analyzed by Two-way ANOVA using Graph Pad Prism Software.

2.3. Molecular docking studies

With the fact that hydrazinecarbothioamide is a key pharmacophore in thioacetazone (TAC) drug, its mechanism of action is still uncertain. Among the target studies TAC is shown to remove *Mycobacterium tuberculosis* interfering in mycolic biosynthesis pathway, the precise number of enzymes involved in this process remains unknown.[16, 17] To understand the probable binding mode of the most active compound **4j**, molecular docking studies were performed against *Mycobacterium tuberculosis* enzymes, enoyl reductase (InhA), PDB ID: 4TZK; Decaprenylphosphoryl-β-d-ribose 2'-epimerase (DprE1), PDB ID: 4P8N; Alcohol dehydrogenase (ADH), PDB ID: 2VHW; (3R)-hydroxyacyl-ACP dehydratase (HadAB), PDB ID:4RV2; Lysine-ε aminotransferase (LAT), PDB ID: 2CJD; Topoisomerase (DNA Gyrase), PDB ID: 5BS8 and Glutamate recemase (MurI), PDB ID: 5H7J. The results of docking studies are described in **Table**

S1 (supporting information). *In silico* studies of **4j** showed good binding energy (-8.313) to the target enzyme enoyl reductase (InhA), whereas co-crystallized inhibitor 1-cyclohexyl-*N*-(3,5-dichlorophenyl)-5-oxopyrrolidine-3-carboxamide showed -10.155 kcal/mol. The binding mode of the target enzyme is confirmed from X-ray with a resolution of 1.62 Å [35,36]. The docking results were drawn based on the docking score, hydrogen bonding and Van der Waals interactions of the ligand with the enzyme (**Figure 8**). The docking results showed that compound **4j** bonded via hydrogen bonding with the P156 residue of the enzyme. InhA is known to catalyze the NADH-dependent reduction of enoyl-ACP in the biosynthesis of fatty and mycolic acids, an essential component of the membrane and cell wall of *M. tuberculosis*.[37] Hence the antitubercular property of compound **4j** could be due to the inhibition of InhA enzyme.

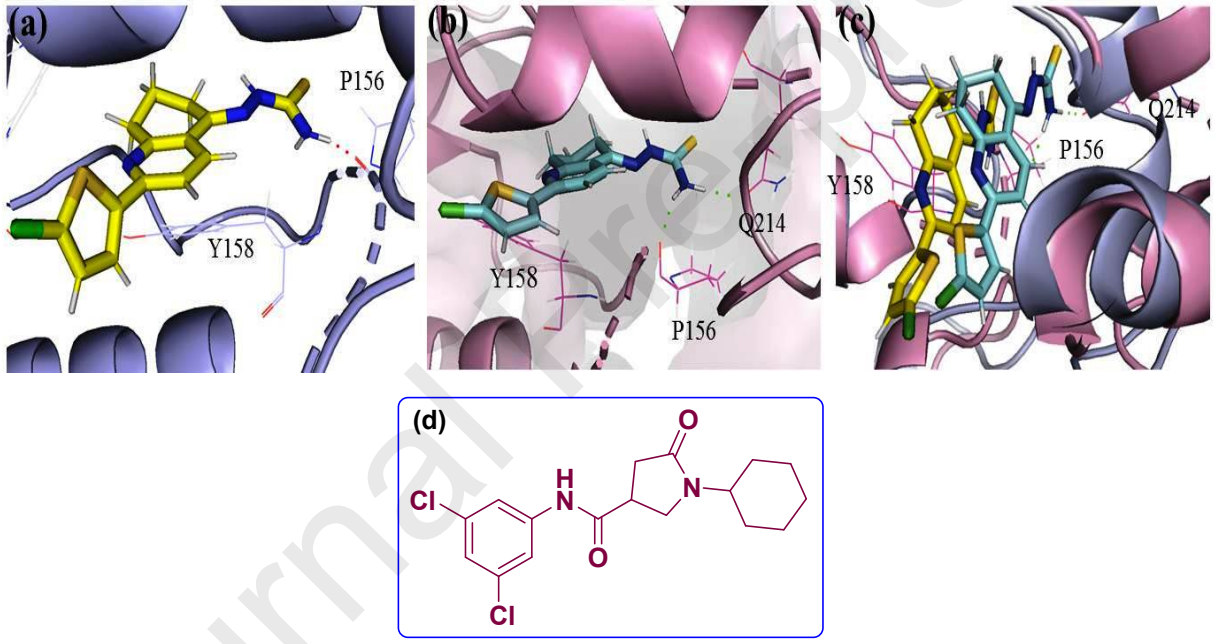

Figure 8: Binding mode of compound **4j** to *Mtb* InhA. (a) The binding mode of **4j** after docking (yellow carbons). (b) The binding of **4j** with target after 50 ns of molecular dynamics simulation with a transparent surface for *Mtb* InhA in the background. (c) Comparison, interactions of test compound **4j** with *Mtb* InhA docking pose (yellow carbon) and after 50 ns of molecular dynamics simulation (cyan carbons). Amino acid side-chains are shown as thin sticks. Ligand bonds to residues are shown as green dashed lines. (d) The chemical structure of 1-cyclohexyl-*N*-(3,5-dichlorophenyl)-5-oxopyrrolidine-3-carboxamide.

2.4. Molecular Dynamics (MD) Simulations

Molecular dynamics (MD) simulation was run for receptor with **4j** complex. The inclusion complex was soaked in explicit solvent water, and MD simulation was run at a temperature of 300 K for a total time period of 50 ns, during which 5208 structural frames of receptor and ligand complex were enumerated, was saved in the trajectory. To access the stability of complex structures computed during MD simulation, the structures from the trajectory aligned to receptor atoms of the first frame and root mean square deviation (RMSD) was calculated for receptor and individual ligand with respect to the initial frame. The complex gets stabilized in the initial phase of MD simulation. So the analysis of the structural stability was carried out on the final phase of 50 ns. Test compound **4j** orientation changed slightly after dynamics and formed an additional hydrogen bond with Q214 residue while retaining the interactions with P156. The key residue Y158 bonded via van der Waals interaction with in the 4 Å regions throughout the 50ns simulations time. Average RMSD values of receptor and **4j** were observed to be 1.9Å and 2.1Å respectively (**Figure 9**) [39,40].

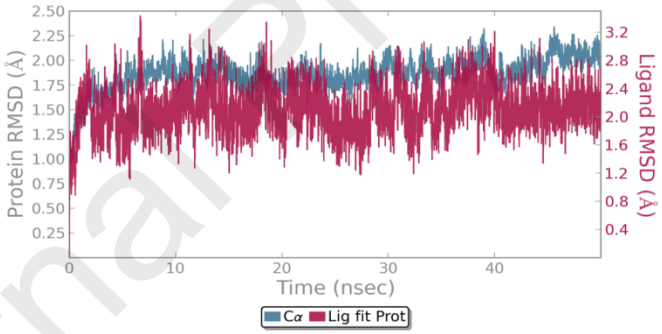

Figure 9: Receptor and compound **4j** RMSD in 50ns time

3. Conclusion

In conclusion, the present study describes the synthesis and evaluation of dihydroquinolin-5(6*H*)-ylidene)hydrazinecarbothioamide derivatives **4a–v** against *M. tuberculosis* H37Rv. Compounds **4a-k** were found to exhibit good antitubercular inhibition (MIC<3.13 µg/mL). Two compounds **4e** and **4j** exhibited the highest inhibition with an MIC of 0.39µg/mL and low cytotoxicity. Hydrazinecarbothioamides **4a-k** exhibited enhanced activity by several times than dihydroquinolinones **3a-k** without hydrazinecarbothioamide. The observed increase in potency

provides clear evidence that hydrazinecarbothioamide is a potential pharmacophore and when coupled to dihydroquinoline, imparts increased antitubercular properties to the molecule. Compounds **4l-v** with gem-dimethyl group and hydrazinecarbothioamide could not induce synergistic effect. The *in vivo* (Zebra fish) antimycobacterial screening of active molecules led to the identification of a hit compound **4j** and exhibited a significant bacterial log reduction in the nutrient starvation model (2.2-fold reduction). Docking studies of **4j** showed a hydrogen bond between the molecule and P156 residue of the target protein. It may be said that the antitubercular property of the molecule could be via the inhibition of InhA enzyme. As part of our global efforts to identify new antitubercular agents the data presented here may serve as foundation for the identified lead compound **4j** for further preclinical and clinical investigations.

4. Experimental Section

All the starting materials and other reagents of the best grade were commercially available and were used without further purification. TLC was performed on Merck 60 F-254 silica gel plates. Spots were visualized by UV light. All melting points were measured by CINTEX programmable melting point apparatus and are uncorrected. ^{1}H and ^{13}C NMR spectra of samples in $CDCl_3$ and DMSO-d_6 were recorded on 75, 100, 300, 400, and 500 MHz spectrometers using tetramethylsilane as the internal standard. Chemical shifts are reported in parts per million (ppm) downfield from tetramethylsilane. Spin multiplicities are described as s (singlet), brs (broad singlet), d (doublet), t (triplet), q (quartet), or m (multiplet). Coupling constants are reported in hertz (Hz). HRMS analyses were acquired on single quadruple and carried out using the ESI techniques at 70 eV. Wherever required column chromatography was performed using silica gel of 60–120 mm with hexane and ethyl acetate as eluents.

4.1. General Procedure for the synthesis of dihydro-6*H*-quinolin-5-ones (3a-v)

The dihydro-6*H*-quinolin-5-one (**3a-v**) were synthesized based on a literature method as following: aryl and heteroaryl methylketones (**1a-k,** 5.23 mmol) were treated with dimethylformamide-dimethylacetal (DMF-DMA) (20.92 mmol) in refluxing xylene for 7 h to form β-enaminones (**2a-k**), and reacted with cyclohexane-1,3-dione/5,5-dimethylcyclohexane-1,3-dione (0.16 g, 1.2 mmol) ammonium acetate (2.0 mmol) in 2-propanol (5 mL) were added $CeCl_3.7H_2O$ (0.2 mmol), NaI (0.2 mmol) and refluxed for 4 h (monitored by TLC). The reaction mixture was cooled to room temperature; a solid precipitate was filtered and washed with cold 2-propanol. The combined solvent was evaporated, and the crude residue obtained was subjected to column chromatography

(hexane: ethyl acetate) to obtain dihydro-6*H*-quinolin-5-one derivatives **(3a-v)** as solids in very good yields.

4.1.1. 2-(4-fluorophenyl)-7,8-dihydroquinolin-5(6*H*)-one (3f)

Light yellow solid, yield 88%, mp: 90-92 °C; ^{1}H NMR (400 MHz, $CDCl_3$): δ 8.31 (d, J = 8.1 Hz, 1H, Ar-H), 8.10-8.02 (m, 2H, Ar-H), 7.65 (d, J = 8.1 Hz, 1H, Ar-H), 7.21-7.13 (m, 2H, Ar-H), 3.20 (t, J = 6.2 Hz, 2H, CH_2), 2.71 (t, J = 6.1 Hz, 2H, CH_2), 2.22 (qt, J = 6.2 Hz, 2H, CH_2); ^{13}C NMR (100 MHz, $CDCl_3$): δ 196.6, 163.3 (d, J = 250.1 Hz, 1C), 163.0, 158.2, 134.9, 133.7 (d, J = 2.2 Hz, 1C), 128.7 (d, J = 8.8 Hz, 2C), 125.6, 117.5, 115.0 (d, J = 22.0 Hz, 2C), 37.7, 32.1, 21.2; MS (ESI): *m/z* 242 $[M+H]^+$; HRMS (ESI) calcd for $C_{15}H_{13}ONF$ $[M+H]^+$ 242.09773; found: 242.09757.

4.1.2. 2-(4-bromophenyl)-7,8-dihydroquinolin-5(6*H*)-one (3h)

Light yellow solid, yield 84%, mp: 124-126 °C; ^{1}H NMR (400 MHz, $CDCl_3$): δ 8.31 (d, J = 8.1 Hz, 1H, Ar-H), 7.96-7.90 (m, 2H, Ar-H), 7.66 (d, J = 8.1 Hz, 1H, Ar-H), 7.63-7.57 (m, 2H, Ar-H), 3.20 (t, J = 6.2 Hz, 2H, CH_2), 2.71 (t, J = 7.0 Hz, 2H, CH_2), 2.22 (qt, J = 6.2 Hz, 2H, CH_2); ^{13}C NMR (100 MHz, $CDCl_3$): δ 178.7, 157.1, 154.6, 145.3, 137.1, 133.2, 131.2, 128.2, 125.8, 122.7, 117.6, 45.6, 37.9, 30.3, 27.8; MS (ESI): *m/z* 302 $[M+H]^+$; HRMS (ESI) calcd for $C_{15}H_{13}ONBr$ $[M+H]^+$ 302.01845; found: 302.01750.

4.1.3. 2-(4-fluorophenyl)-7,7-dimethyl-7,8-dihydroquinolin-5(6*H*)-one (3q)

Light yellow solid, yield 90%, mp: 96-98 °C; ^{1}H NMR (400 MHz, $CDCl_3$): δ 8.30 (d, J = 8.1 Hz, 1H, Ar-H), 8.10-8.03 (m, 2H, Ar-H), 7.66 (d, J = 8.1 Hz, 1H, Ar-H), 7.22-7.14 (m, 2H, Ar-H), 3.09 (s, 2H, CH_2), 2.57 (s, 2H, CH_2), 1.14 (s, 6H, $2CH_3$); ^{13}C NMR (100 MHz, $CDCl_3$): δ 196.8, 163.5 (d, J = 250.1 Hz, 1C), 161.7, 158.9, 134.7, 133.9 (d, J = 2.2 Hz, 1C), 128.8 (d, J = 8.8 Hz, 2C), 128.8, 124.9, 117.6, 115.2 (d, J = 21.2 Hz, 2C), 51.4, 46.0, 32.3, 27.7; MS (ESI): *m/z* 270 $[M+H]^+$; HRMS (ESI) calcd for $C_{16}H_{17}N_4S$ $[M+H]^+$ 270.12933; found: 270.12887.

4.2. General Procedure for the synthesis of dihydroquinolin-5(6*H*)-ylidene)hydrazine carbothioamide derivatives (4a-v)

A mixture of dihydro-6*H*-quinolin-5-one **(3a-v)** (1.0 mmol), thiosemicarbazide (1.1 mmol) and catalytic amount of sulphuric acid in methanol (10 mL) were refluxed for 4-5 h. After completion, (monitored on TLC), the reaction product was cooled, precipitate was filtered and the dried residue was recrystalized by using methanol to afford compound **(4a-v)** as solids in excellent yields.

4.2.1. (*E*)-2-(2-phenyl-7,8-dihydroquinolin-5(6*H*)-ylidene)hydrazinecarbothioamide (4a)

Colorless solid, yield 0.42 g, 92%, mp: 246-248 °C; ^{1}H NMR (300 MHz, DMSO-d_6): δ 9.62 (br s, 1H, NH), 8.42 (d, J = 8.3 Hz, 1H, Ar-H), 8.14-8.03 (m, 2H, Ar-H), 7.73 (br s, 1H, NH), 7.67-7.54 (m, 2H, Ar-H), 7.52-7.41 (m, 3H, Ar-H), 3.04 (t, J = 5.8 Hz, 2H, CH_2), 2.73 (t, J = 6.4 Hz, 2H, CH_2), 2.07 (qt, J = 5.8 Hz, 2H, CH_2); ^{13}C NMR (75 MHz, $CDCl_3$+DMSO-d_6): δ 178.6, 158.4, 155.8, 146.0, 138.0, 133.0, 128.6, 128.1, 126.2, 125.9, 117.8, 31.9, 24.8, 20.4; IR (KBr) 3423, 3244, 3147, 2948, 1578, 1497, 1456, 1447, 1283, 1105, 1081, 839, 749, 695 cm^{-1}; MS (ESI): *m/z* 297 $[M+H]^+$. HRMS (ESI) calcd for $C_{16}H_{17}N_4S$ $[M+H]^+$ 297.11627; found: 297.11684.

4.2.2. (*E*)-2-(2-*p*-tolyl-7,8-dihydroquinolin-5(6*H*)-ylidene)hydrazinecarbothioamide (4b)

Colorless solid, yield 0.40 g, 89%, mp: 260-262 °C; ^{1}H NMR (300 MHz, DMSO-d_6): δ 10.25 (br s, 1H, NH), 8.85 (d, J = 8.3 Hz, 1H, Ar-H), 8.29 (br s, 1H, NH), 8.04 (br s, 1H, NH), 8.01-7.94 (m, 2H, Ar-H), 7.76 (d, J = 8.3 Hz, 1H, Ar-H), 7.46-7.31 (m, 2H, Ar-H), 3.06 (t, J = 5.8 Hz, 2H, CH_2), 2.78 (t, J = 6.2 Hz, 2H, CH_2), 2.42 (s, 3H, CH_3), 2.02 (qt, J = 5.8 Hz, 2H, CH_2); ^{13}C NMR (75 MHz, $CDCl_3$+DMSO-d_6): δ 178.7, 157.1, 154.2, 144.7, 139.5, 135.6, 133.2, 129.1, 127.0, 126.8, 118.8, 30.6, 24.8, 20.7, 20.0; IR (KBr) 3404, 3381, 3202, 3137, 2945, 1584, 1506, 1455, 1412, 1293, 1082, 815, 751, 674 cm^{-1}; MS (ESI): *m/z* 311 $[M+H]^+$. HRMS (ESI) calcd for $C_{17}H_{19}N_4S$ $[M+H]^+$ 311.13205; found: 311.13249.

4.2.3. (*E*)-2-(2-(4-methoxyphenyl)-7,8-dihydroquinolin-5(6*H*)-ylidene)hydrazinecarbothioamide (4c)

Colorless solid, yield: 0.38 g, 86%; mp; 238-240 ^{0}C ^{1}H NMR (300 MHz, DMSO-d_6): δ 10.22 (br s, 1H, NH), 8.72 (d, J = 8.3 Hz, 1H, Ar-H), 8.28 (br s, 1H, NH), 8.08-7.97 (m, 3H, Ar-H), 7.69 (d, J = 8.3 Hz, 1H, Ar-H), 7.10-6.96 (m, 2H, Ar-H), 3.85 (s, 3H, OCH_3), 2.98 (t, J = 5.4 Hz, 2H, CH_2), 2.76 (t, J = 6.0 Hz, 2H, CH_2), 1.98 (qt, J = 5.6 Hz, 2H, CH_2); ^{13}C NMR (75 MHz, $CDCl_3$ + DMSO-d_6): δ 178.7, 160.5, 157.7, 154.6, 145.7, 134.8, 129.4, 128.3, 126.1, 118.0, 114.0, 55.1, 31.3, 25.0, 20.3; IR (KBr) 3422, 3245, 3149, 2931, 1625, 1603, 1588, 1504, 1455, 1243, 1175, 1026, 822, 673 cm^{-1}; MS (ESI): *m/z* 327 $[M+H]^+$; HR-MS (ESI) Calcd for $C_{17}H_{19}N_4OS$ $[M+H]^+$: 327.12691, found: 327.12741.

4.2.4. (*E*)-2-(2-(biphenyl-4-yl)-7,8-dihydroquinolin-5(6*H*)-ylidene)hydrazinecarbothioamide (4d)

Colorless solid, yield: 0.38 g, 88%; mp: 252-254 ^{0}C ^{1}H NMR (300 MHz, DMSO-d_6): δ 10.32 (br s, 1H, NH), 8.80 (d, J = 8.3 Hz, 1H, Ar-H), 8.36 (br s, 1H, NH), 8.29-8.17 (m, 3H, Ar-H), 7.87 (d, J = 8.3 Hz, 1H, Ar-H), 7.83-7.71 (m, 4H, Ar-H), 7.56-7.45 (m, 2H, Ar-H), 7.40-7.32 (m, 1H, Ar-

H), 2.96 (t, *J* = 5.6 Hz, 2H, CH_2), 2.75 (t, *J* = 6.0 Hz, 2H, CH_2), 1.93 (qt, *J* = 5.6 Hz, 2H, CH_2); ^{13}C NMR (75 MHz, DMSO-d_6): δ 178.7, 158.6, 154.8, 146.2, 140.7, 139.3, 136.9, 134.0, 128.9, 127.6, 127.1, 126.8, 126.5, 118.0, 32.0, 25.1, 20.5; IR (KBr) 3407, 3223, 3139, 1587, 1496, 1455, 1293, 1105, 1080, 847, 761, 693 cm^{-1}; MS (ESI): *m/z* 373 $[M+H]^+$; HR-MS (ESI) Calcd for $C_{22}H_{21}N_4S$ $[M+H]^+$: 373.14847, found: 373.14814.

4.2.5. (*E*)-2-(2-(naphthalen-2-yl)-7,8-dihydroquinolin-5(6*H*)-ylidene)hydrazinecarbothioamide (4e)

Colorless solid, yield: 0.36 g, 82%; mp: 224-226 ^{0}C; ^{1}H NMR (300 MHz, DMSO-d_6): δ 10.33 (br s, 1H, NH), 8.91 (d, *J* = 8.2 Hz, 1H, Ar-H), 8.66 (br s, 1H, NH), 8.38 (br s, 1H, NH), 8.30-8.14 (m, 2H, Ar-H), 8.09-7.92 (m, 4H, Ar-H), 7.60-7.53 (m, 2H, Ar-H), 3.05 (t, *J* =5.5 Hz, 2H, CH_2), 2.79 (t, *J* = 6.0 Hz, 2H, CH_2), 1.99 (qt, *J* = 5.5 Hz, 2H, CH_2); ^{13}C NMR (75 MHz, $CDCl_3$ + DMSO-d_6): δ 178.8, 156.8, 154.4, 145.3, 135.0, 134.1, 133.2, 132.7, 128.5, 128.1, 127.3, 127.0, 126.8, 126.4, 126.3, 124.2, 119.1, 31.2, 25.0, 20.2; IR (KBr) 3249, 3144, 1578, 1494, 1449, 1249, 1214, 1109, 995, 847, 752, 672 cm^{-1}; MS (ESI): *m/z* 347 $[M+H]^+$; HR-MS (ESI) Calcd for $C_{20}H_{19}N_4S$ $[M+H]^+$: 347.13250, found: 347.13249.

4.2.6. (*E*)-2-(2-(4-fluorophenyl)-7,8-dihydroquinolin-5(6*H*)-ylidene)hydrazinecarbothioamide (4f)

Colorless solid, yield: 0.36 g, 80%; mp: 232-234 ^{0}C; 1H NMR (300 MHz, DMSO-d_6): δ 10.25 (br s, 1H, NH), 8.74 (d, *J* = 8.4 Hz, 1H, Ar-H), 8.32 (br s, 1H, NH), 8.21-8.05 (m, 3H, Ar-H), 7.74 (d, *J* = 8.4 Hz, 1H, Ar-H), 7.24 (m, 2H, Ar-H), 2.96 (t, *J* = 5.8 Hz, 2H, CH_2), 2.76 (t, *J* = 6.2 Hz, 2H, CH_2), 1.96 (qt, *J* = 5.8 Hz, 2H, CH_2); 13C NMR (75 MHz, $CDCl_3$ + DMSO-d_6) δ: 178.6, 162.7 (d, *J* = 247.0 Hz, 1C), 158.3, 154.2, 145.9, 134.4 (d, *J* = 2.2 Hz, 1C), 133.7, 128.5 (d, *J* = 8.2 Hz, 2C), 126.2, 117.6, 115.1 (d, *J* = 21.4 Hz, 2C), 31.9, 25.0, 20.4; IR (KBr) 3234, 3140, 1586, 1503, 1456, 1292, 1227, 1159, 1079, 826, 772, 673 cm^{-1}; MS (ESI): m/z 315 [M+H]+; HR-MS (ESI): Calcd for $C_{16}H_{16}N_4FS$ $[M+H]^+$ 315.10696, found: 315.10742.

4.2.7. (*E*)-2-(2-(4-chlorophenyl)-7,8-dihydroquinolin-5(6*H*)-ylidene)hydrazinecarbothioamide (4g)

Colorless solid , yield: 0.37 g, 83%. mp: 266-268 ^{0}C; ^{1}H NMR (300 MHz, DMSO-d_6): δ 10.24 (br s, 1H, NH), 8.73 (d, *J* = 8.3 Hz, 1H, Ar-H), 8.31 (br s, 1H, NH), 8.20-8.03 (m, 3H, Ar-H), 7.75 (d, *J* = 8.3 Hz, 1H, Ar-H), 7.56-7.46 (m, 2H, Ar-H), 2.97 (t, *J* = 5.8 Hz, 2H, CH_2), 2.76 (t, *J* = 6.2 Hz, 2H, CH_2), 1.97 (qt, *J* = 5.8 Hz, 2H, CH_2); ^{13}C NMR (75 MHz, $CDCl_3$ + DMSO-d_6): δ 178.7, 158.4,

154.0, 145.8, 136.7, 134.0, 133.7, 128.3, 128.0, 126.6, 117.8, 32.0, 25.0, 20.4; IR (KBr) 3424, 3237, 3145, 2949, 1579, 1496, 1453, 1413, 1285, 1215, 1091, 844, 754 cm^{-1}; MS (ESI): *m/z* 331 $[M+H]^+$; HR-MS (ESI) Calcd for $C_{16}H_{16}N_4ClS$ $[M+H]^+$: 331.07795, found: 331.07787.

4.2.8. (*E*)-2-(2-(4-bromophenyl)-7,8-dihydroquinolin-5(6*H*)-ylidene)hydrazinecarbothioamide (4h)

Colorless solid, yield: 0.35 g, 81%; mp: 278-280 ^0C; ^1H NMR (300 MHz, DMSO-d_6): δ 10.28 (br s, 1H, NH), 8.76 (d, *J* = 8.3 Hz, 1H, Ar-H), 8.33 (br s, 1H, NH), 8.18-7.98 (m, 3H, Ar-H), 7.78 (d, *J* = 8.3 Hz, 1H, Ar-H), 7.72-7.62 (m, 2H, Ar-H), 2.96 (t, *J* = 5.8 Hz, 2H, CH_2), 2.76 (t, *J* = 6.2 Hz, 2H, CH_2), 1.95 (qt, *J* = 5.8 Hz, 2H, CH_2); ^{13}C NMR (75 MHz, $CDCl_3$ + DMSO-d_6): δ 178.7, 158.5, 154.0, 145.8, 137.1, 133.8, 131.3, 128.3, 126.7, 122.7, 117.8, 31.9, 25.0, 20.4; IR (KBr) 3423, 3228, 3144, 1594, 1579, 1453, 1291, 1215, 1082, 846, 769, 663 cm^{-1}; MS (ESI): *m/z* 375 $[M+H]^+$; HR-MS (ESI) Calcd for $C_{16}H_{16}N_4BrS$ $[M+H]^+$: 375.02610, found: 375.02736.

4.2.9. (*E*)-2-(2-(thiophen-2-yl)-7,8-dihydroquinolin-5(6*H*)-ylidene)hydrazinecarbothioamide (4i)

Colorless solid, yield: 0.39 g, 85%; mp: 226-228 ^0C; ^1H NMR (300 MHz, DMSO-d_6): δ 10.16 (br s, 1H, NH), 8.61 (d, *J* = 8.2 Hz, 1H, Ar-H), 8.28 (br s, 1H, NH), 8.03 (br s, 1H, NH), 7.75 (dd, *J* = 3.5, 0.8 Hz, 1H, Ar-H), 7.61 (d, *J* = 8.2 Hz, 1H, Ar-H), 7.54 (dd, *J* = 4.9, 0.8 Hz, 1H, Ar-H), 7.13 (dd, *J* = 4.9, 3.5 Hz, 1H, Ar-H), 2.86 (t, *J* = 5.7 Hz, 2H, CH_2), 2.70 (t, *J* = 6.3 Hz, 2H, CH_2), 1.91 (qt, *J* = 5.7 Hz, 2H, CH_2); ^{13}C NMR (75 MHz, $CDCl_3$ + DMSO-d_6): δ 178.6, 158.4, 151.1, 145.9, 144.0, 133.6, 128.4, 128.0, 126.0, 125.4, 116.6, 31.7, 25.0, 20.4; IR (KBr) 3415, 3248, 3148, 2948, 1577, 1492, 1456, 1428, 1279, 1082, 858, 751, 663 cm^{-1}; MS (ESI): *m/z* 303 $[M+H]^+$; HR-MS (ESI) Calcd for $C_{14}H_{15}N_4S_2$ $[M+H]^+$: 303.07308, found: 303.07326.

4.2.10. (*E*)-2-(2-(5-chlorothiophen-2-yl)-7,8-dihydroquinolin-5(6*H*)ylidene)hydrazinecarbothioamide (4j)

Colorless solid, yield: 0.38 g, 86%. mp: 236-238 ^0C; ^1H NMR (300 MHz, DMSO-d_6): δ 10.13 (br s, 1H, NH), 8.59 (d, *J* = 8.3 Hz, 1H, Ar-H), 8.22 (br s, 1H, NH), 7.93 (br s, 1H, NH), 7.58 (d, *J* = 8.3 Hz, 1H, Ar-H), 7.53 (d, *J* = 3.9 Hz, 1H, Ar-H), 7.00 (d, *J* = 3.9 Hz, 1H, Ar-H), 2.90 (t, *J* = 6.0 Hz, 2H, CH_2), 2.74 (t, *J* = 6.2 Hz, 2H, CH_2), 1.98 (qt, *J* = 6.0 Hz, 2H, CH_2); ^{13}C NMR (75 MHz, $CDCl_3$ + DMSO-d_6): δ 178.7, 158.5, 150.2, 145.8, 143.2, 133.8, 131.0, 128.0, 126.6, 125.2, 116.1, 31.6, 25.0, 20.3; IR (KBr) 3416, 3222, 3134, 2944, 1586, 1502, 1458, 1430, 1294, 1097, 838, 794,

764 cm^{-1}; MS (ESI): *m/z* 337 $[M+H]^+$; HR-MS (ESI) Calcd for $C_{14}H_{14}ClN_4S_2$ $[M+H]^+$: 337.03414, found: 337.03429.

4.2.11. (*E*)-2-(2-(5-bromothiophen-2-yl)-7,8-dihydroquinolin-5(6*H*)-ylidene)hydrazinecarbothioamide (4k)

Colorless solid, yield: 0.35 g, 83%. mp: 218-220 ^{0}C; ^{1}H NMR (300 MHz, DMSO-d_6): δ 10.27 (br s, 1H, NH), 8.74 (d, *J* = 8.5 Hz, 1H, Ar-H), 8.33 (br s, 1H, NH), 8.18 (br s, 1H, NH), 7.80-7.69 (m, 2H, Ar-H), 7.30-7.24 (m, 1H, Ar-H), 2.85 (t, *J* = 5.7 Hz, 2H, CH_2), 2.71 (t, *J* = 6.0 Hz, 2H, CH_2), 1.88 (qt, *J* = 5.7 Hz, 2H, CH_2); ^{13}C NMR (75 MHz, DMSO-d_6): δ 178.7, 158.6, 150.1, 145.9, 145.5, 134.4, 131.9, 126.8, 126.7, 116.6, 115.0, 31.5, 25.1, 20.4; IR (KBr) 3415, 3223, 3136, 2948, 1585, 1502, 1457, 1425, 1292, 1099, 827, 795, 663 cm^{-1}; MS (ESI): *m/z* 380 $[M+H]^+$; HR-MS (ESI) Calcd for $C_{14}H_{14}BrN_4S_2$ $[M+H]^+$: 380.98369, found: 380.98378.

4.2.12. (*E*)-2-(7,7-dimethyl-2-phenyl-7,8-dihydroquinolin-5(6*H*)ylidene)hydrazinecarbothioamide (4l)

Colorless solid, yield: 0.38 g, 85%; mp: 230-232 ^{0}C; ^{1}H NMR (300 MHz, DMSO-d_6): δ 10.17 (br s, 1H, NH), 8.65 (d, *J* = 8.2 Hz, 1H, Ar-H), 8.22 (br s, 1H, NH), 8.08-7.94 (m, 3H, Ar-H), 7.66 (d, *J* = 8.2 Hz, 1H, Ar-H), 7.48-7.34 (m, 3H, Ar-H), 2.83 (s, 2H, CH_2), 2.59 (s, 2H, CH_2), 1.02 (s, 6H, $2CH_3$); ^{13}C NMR (75 MHz, $CDCl_3$ + DMSO-d_6): δ 178.6, 157.0, 155.9, 145.4, 138.0, 133.0, 128.7, 128.2, 126.3, 125.4, 117.6, 45.6, 37.9, 30.3, 27.8; IR (KBr) 3409, 3249, 3149, 2952, 1588, 1493, 1441, 1289, 1079, 853, 782, 688 cm^{-1}; MS (ESI): m/z 325 $[M+H]^+$; HR-MS (ESI) Calcd for $C_{18}H_{21}N_4S$ $[M+H]^+$: 325.14840, found: 325.14814.

4.2.13. (*E*)-2-(7,7-dimethyl-2-p-tolyl-7,8-dihydroquinolin-5(6*H*)-ylidene)hydrazinecarbothioamide (4m)

Colorless solid, yield: 0.34 g, 78%; mp: 244-246 ^{0}C; ^{1}H NMR (300 MHz, DMSO-d_6): δ 10.28 (br s, 1H, NH), 8.76 (d, *J* = 8.2 Hz, 1H, Ar-H), 8.33 (br s, 1H, NH), 8.13 (br s, 1H, NH), 8.08-7.98 (m, 2H, Ar-H), 7.77 (d, *J* = 8.2 Hz, 1H, Ar-H), 7.36-7.26 (m, 2H, Ar-H), 2.84 (s, 2H, CH_2), 2.63 (s, 2H, CH_2), 2.36 (s, 3H, CH_3), 1.00 (s, 6H, $2CH_3$); 13C NMR (75 MHz, $CDCl_3$ + DMSO-d_6): δ 178.7, 157.1, 155.9, 145.7, 138.6, 135.3, 133.3, 129.1, 126.3, 125.3, 117.5, 45.7, 38.0, 30.4, 27.9, 20.8; IR (KBr) 3426, 3251, 3154, 2954, 1589, 1493, 1452, 1440, 1293, 1183, 1075, 818, 750, 673 cm^{-1}; MS (ESI): m/z 339 $[M+H]^+$; HR-MS (ESI) Calcd for $C_{19}H_{23}N_4S$ $[M+H]^+$: 339.16405, found: 339.16379.

4.2.14. (*E*)-2-(2-(4-methoxyphenyl)-7,7-dimethyl-7,8-dihydroquinolin-5(6*H*)ylidene)hydrazinecarbothioamide (4n)

Colorless solid, yield: 0.35 g, 81%; mp; 226-228 ^{0}C ^{1}H NMR (300 MHz, DMSO-d$_6$): δ 10.14 (br s, 1H, NH), 8.60 (d, *J* = 8.2 Hz, 1H, Ar-H), 8.20 (br s, 1H, NH), 8.03-7.88 (m, 3H, Ar-H), 7.59 (d, *J* = 8.2 Hz, 1H, Ar-H), 6.95-7.05 (m, 2H, Ar-H), 3.80 (s, 3H, OCH_3), 2.80 (s, 2H, CH_2), 2.57 (s, 2H, CH_2), 1.01 (s, 6H, $2CH_3$); ^{13}C NMR (75 MHz, $CDCl_3$ + DMSO-d$_6$): δ 178.6, 160.1, 156.8, 155.5, 145.6, 133.2, 130.3, 127.8, 124.7, 117.0, 113.7, 54.9, 45.6, 37.9, 30.4, 27.8; IR (KBr) 3427, 3250, 3154, 2956, 1579, 1492, 1453, 1293, 1247, 1179, 1075, 847, 751, 673 cm^{-1}; MS (ESI): *m/z* 355 $[M+H]^+$; HR-MS (ESI) Calcd for $C_{19}H_{23}N_4OS$ $[M+H]^+$: 355.15919, found: 355.15871.

4.2.15. (*E*)-2-(2-(biphenyl-4-yl)-7,7-dimethyl-7,8-dihydroquinolin-5(6*H*)-ylidene)hydrazine carbothioamide (4o)

Colorless solid, yield: 0.33 g, 79%; mp: 218-220 ^{0}C ^{1}H NMR (300 MHz, DMSO-d$_6$): δ 10.32 (br s, 1H, NH), 8.83 (d, *J* = 8.2 Hz, 1H, Ar-H), 8.37 (br s, 1H, NH), 8.29-8.17 (m, 3H, Ar-H), 7.88 (d, *J* = 8.2 Hz, 1H, Ar-H), 7.84-7.67 (m, 4H, Ar-H), 7.58-7.48 (m, 2H, Ar-H), 7.46-7.38 (m, 1H, Ar-H), 2.87 (s, 2H, CH_2), 2.65 (s, 2H, CH_2), 1.01 (s, 6H, $2CH_3$); ^{13}C NMR (75 MHz, DMSO-d$_6$): δ 178.7, 157.1, 155.1, 145.5, 140.7, 139.2, 136.7, 133.8, 128.8, 127.6, 127.1, 126.7, 126.5, 125.9, 118.0, 45.4, 37.9, 30.4, 27.8; IR (KBr) 3425, 3250, 3150, 2955, 1579, 1493, 1452, 1282, 1075, 830, 753, 665 cm^{-1}; MS (ESI): *m/z* 401 $[M+H]^+$; HR-MS (ESI) Calcd for $C_{24}H_{25}N_4S$ $[M+H]^+$: 401.17995, found: 401.17944.

4.2.16. (*E*)-2-(7,7-dimethyl-2-(naphthalen-2-yl)-7,8-dihydroquinolin-5(6*H*)-ylidene)hydrazinecarbothioamide (4p)

Colorless solid, yield: 0.36 g, 84%; mp: 242-244 ^{0}C; ^{1}H NMR (300 MHz, DMSO-d$_6$): δ 10.27 (br s, 1H, NH), 8.78 (d, *J* = 8.2 Hz, 1H, Ar-H), 8.64 (br s, 1H, NH), 8.37-8.23 (m, 2H, Ar-H), 8.13 (br s, 1H, NH), 8.04-7.85 (m, 4H, Ar-H), 7.56-7.48 (m, 2H, Ar-H), 2.89 (s, 2H, CH_2), 2.64 (s, 2H, CH_2), 1.04 (s, 6H, $2CH_3$); ^{13}C NMR (75 MHz, $CDCl_3$ + DMSO-d$_6$): δ 178.7, 157.2, 155.5, 145.5, 135.4, 133.3, 133.1, 132.8, 128.4, 127.9, 127.2, 126.4, 126.1, 125.76, 125.70, 124.1, 118.1, 45.7, 37.9, 30.4, 27.8; IR (KBr) 3411, 3241, 3144, 2950, 1584, 1496, 1448, 1291, 1077, 855, 750, 673 cm^{-1}; MS (ESI): *m/z* 375 $[M+H]^+$; HR-MS (ESI) Calcd for $C_{22}H_{23}N_4S$ $[M+H]^+$: 375.16444, found: 375.16379.

4.2.17. (*E*)-2-(2-(4-fluorophenyl)-7,7-dimethyl-7,8-dihydroquinolin-5(6*H*)-ylidene)hydrazine carbothioamide (4q)

Colorless solid, yield: 0.36 g, 82%; mp: 244-246 ^{0}C; 1H NMR (300 MHz, DMSO-d_6): δ 10.26 (br s, 1H, NH), 8.74 (d, *J* = 8.5 Hz, 1H, Ar-H), 8.32 (br s, 1H, NH), 8.19-8.09 (m, 3H, Ar-H), 7.74 (d, *J* = 8.5 Hz, 1H, Ar-H), 7.29-7.20 (m, 2H, Ar-H), 2.82 (s, 2H, CH_2), 2.61 (s, 2H, CH_2), 1.06 (s, 6H, $2CH_3$); 13C NMR (75 MHz, DMSO-d_6) δ: 178.7, 162.8 (d, *J* = 246.4 Hz, 1C), 157.2, 154.7, 145.6, 134.5 (d, *J* = 2.2 Hz, 1C), 133.6, 128.7 (d, *J* = 8.8 Hz, 2C), 125.6, 117.7, 115.4 (d, *J* = 21.4 Hz, 2C), 45.6, 37.9, 30.4, 27.8; IR (KBr) 3401, 3223, 3146, 2953, 1584, 1496, 1452, 1291, 1214, 1073, 748, 670 cm^{-1}; MS (ESI): m/z 343 [M+H]+; HR-MS (ESI): Calcd for $C_{18}H_{20}N_4FS$ $[M+H]^+$ 343.13911, found: 343.13872.

4.2.18.(*E*)-2-(2-(4-chlorophenyl)-7,7-dimethyl-7,8-dihydroquinolin-5(6*H*)-ylidene)hydrazine carbothioamide (4r)

Colorless solid, yield: 0.34 g, 82%. mp: 248-250 ^{0}C; ^{1}H NMR (300 MHz, DMSO-d_6): δ 10.32 (br s, 1H, NH), 8.81 (d, *J* = 8.3 Hz, 1H, Ar-H), 8.37 (br s, 1H, NH), 8.26-8.12 (m, 3H, Ar-H), 7.84 (d, *J* = 8.3 Hz, 1H, Ar-H), 7.62-7.52 (m, 2H, Ar-H), 2.84 (s, 2H, CH_2), 2.64 (s, 2H, CH_2), 1.00 (s, 6H, $2CH_3$); ^{13}C NMR (75 MHz, DMSO-d_6): δ 178.8, 157.5, 154.6, 145.8, 136.9, 134.1, 133.7, 128.7, 128.3, 126.1, 118.1, 45.7, 38.0, 30.5, 27.9; IR (KBr) 3406, 3248, 3148, 2954, 1587, 1497, 1450, 1288, 1089, 853, 751 cm^{-1}; MS (ESI): *m/z* 359 $[M+H]^+$; HR-MS (ESI) Calcd for $C_{18}H_{20}N_4ClS$ $[M+H]^+$: 359.10932, found: 359.10917.

4.2.19. (*E*)-2-(2-(4-bromophenyl)-7,7-dimethyl-7,8-dihydroquinolin-5(6*H*)-ylidene) hydrazine carbothioamide (4s)

Colorless solid, yield: 0.29 g, 78%; mp: 226-228 ^{0}C; ^{1}H NMR (300 MHz, DMSO-d_6): δ 10.20 (br s, 1H, NH), 8.66 (d, *J* = 8.5 Hz, 1H, Ar-H), 8.24 (br s, 1H, NH), 8.04-7.95 (m, 3H, Ar-H), 7.68 (d, *J* = 8.5 Hz, 1H, Ar-H), 7.60-7.52 (m, 2H, Ar-H), 2.81 (s, 2H, CH_2), 2.58 (s, 2H, CH_2), 1.00 (s, 6H, $2CH_3$); ^{13}C NMR (75 MHz, $CDCl_3$ + DMSO-d_6): δ 178.7, 157.1, 154.6, 145.3, 137.1, 133.2, 131.2, 128.2, 125.8, 122.7, 117.6, 45.6, 37.9, 30.3, 27.8; IR (KBr) 3427, 3249, 3147, 2956, 2337, 1577, 1496, 1449, 1281, 1074, 823, 764, 663 cm^{-1}; MS (ESI): *m/z* 403 $[M+H]^+$; HR-MS (ESI) Calcd for $C_{18}H_{20}N_4BrS$ $[M+H]^+$: 403.05950, found: 403.05866.

4.2.20. (*E*)-2-(7,7-dimethyl-2-(thiophen-2-yl)-7,8-dihydroquinolin-5(6*H*)-ylidene)hydrazine carbothioamide (4t)

Colorless solid, yield: 0.43 g, 80%; mp: 236-238 ^{0}C; ^{1}H NMR (300 MHz, DMSO-d_6): δ 10.28 (br s, 1H, NH), 8.73 (d, *J* = 8.3 Hz, 1H, Ar-H), 8.35 (br s, 1H, NH), 8.19 (br s, 1H, NH), 7.87 (dd, *J* = 3.9, 0.9 Hz, 1H, Ar-H), 7.75 (d, *J* = 8.3 Hz, 1H, Ar-H), 7.65 (dd, *J* = 4.9, 0.9 Hz, 1H, Ar-H), 7.17

(dd, *J* = 4.9, 3.9 Hz, 1H, Ar-H), 2.77 (s, 2H, CH_2), 2.61 (s, 2H, CH_2), 0.99 (s, 6H, $2CH_3$); ^{13}C NMR (75 MHz, DMSO-d_6): δ 178.7, 157.3, 151.7, 145.7, 144.1, 133.4, 128.8, 128.4, 125.8, 125.4, 116.6, 45.3, 37.9, 30.4, 27.8; IR (KBr) 3406, 3248, 3146, 2952, 1586, 1495, 1453, 1288, 1104, 1078, 845, 710, 663 cm^{-1}; MS (ESI): *m/z* 331 $[M+H]^+$; HR-MS (ESI) Calcd for $C_{16}H_{19}N_4S_2$ $[M+H]^+$: 331.10422, found: 331.10456.

4.2.21. (*E*)-2-(2-(5-chlorothiophen-2-yl)-7,7-dimethyl-7,8-dihydroquinolin-5(6*H*)-ylidene)hydrazinecarbothioamide (4u)

Colorless solid, yield: 0.32 g, 82%. mp:243-245 ^{0}C; ^{1}H NMR (300 MHz, DMSO-d_6): δ 10.30 (br s, 1H, NH), 8.76 (d, *J* = 8.2 Hz, 1H, Ar-H), 8.36 (br s, 1H, NH), 8.21 (br s, 1H, NH), 7.81-7.73 (m, 2H, Ar-H), 7.19 (d, *J* = 4.1 Hz, 1H, Ar-H), 2.75 (s, 2H, CH_2), 2.60 (s, 2H, CH_2), 0.98 (s, 6H, $2CH_3$); ^{13}C NMR (75 MHz, $CDCl_3$ + DMSO-d_6): δ 178.6, 157.0, 150.7, 145.2, 143.1, 133.1, 131.1, 127.5, 125.6, 124.5, 115.8, 45.2, 37.8, 30.2, 27.7; IR (KBr) 3404, 3242, 3146, 1589, 1496, 1455, 1288, 1106, 1031, 850, 789, 756, 638 cm^{-1}; MS (ESI): *m/z* 365 $[M+H]^+$; HR-MS (ESI) Calcd for $C_{16}H_{18}N_4S_2Cl$ $[M+H]^+$: 365.06623, found: 365.06559.

4.2.22. (*E*)-2-(2-(5-bromothiophen-2-yl)-7,7-dimethyl-7,8-dihydroquinolin-5(6*H*)-ylidene)hydrazinecarbothioamide (4v)

Colorless solid, yield: 0.30 g, 81%. mp: 252-254 ^{0}C; ^{1}H NMR (300 MHz, DMSO-d_6): δ 10.18 (br s, 1H, NH), 8.63 (d, *J* = 8.5 Hz, 1H, Ar-H), 8.24 (br s, 1H, NH), 8.01 (br s, 1H, NH), 7.78-7.62 (m, 2H, Ar-H), 7.12 (d, *J* = 3.8 Hz, 1H, Ar-H), 2.73 (s, 2H, CH_2), 2.56 (s, 2H, CH_2), 0.99 (s, 6H, $2CH_3$); ^{13}C NMR (75 MHz, $CDCl_3$ + DMSO-d_6): δ 178.6, 157.0, 150.6, 145.8, 145.2, 133.1, 131.0, 125.6, 125.4, 115.8, 114.5, 45.1, 37.8, 30.2, 27.7; IR (KBr) 3405, 3240, 3146, 2955, 1575, 1494, 1454, 1283, 1105, 1072, 848, 756, 663 cm^{-1}; MS (ESI): *m/z* 409 $[M+H]^+$; HR-MS (ESI) Calcd for $C_{16}H_{18}N_4S_2Br$ $[M+H]^+$: 409.01561; found: 409.01508.

4.3. *Antitubercular evaluation assay*

All the compounds were further screened for in vitro antimycobacterial activity against *M. Tuberculosis* H37Rv strain by microplate Alamar blue assay method. Briefly, the inoculum was prepared from fresh LJ medium re-suspended in 7H9-S medium (7H9 broth, 0.1% casitone, 0.5% glycerol, supplemented oleic acid, albumin, dextrose, and catalase [OADC]), adjusted to a McFarland tube No. 1, and diluted 1:20; 100 µl was used as inoculum. Each drug stock solution was thawed and diluted in 7H9-S at four-fold the final highest concentration tested. Serial two-

fold dilutions of each drug were prepared directly in a sterile 96-well microtiter plate using 100 µl 7H9-S. A growth control containing no antibiotic and a sterile control were also prepared on each plate. Sterile water was added to all perimeter wells to avoid evaporation during the incubation. The plate was covered, sealed in plastic bags and incubated at 37°C in normal atmosphere. After 7 days incubation, 30 ml of Alomar blue solution was added to each well, and the plate was re-incubated overnight. A change in color from blue (oxidized state) to pink (reduced) indicated the growth of bacteria, and the MIC was defined as the lowest concentration of drug that prevented this change in color.

4.4. ***Evaluation of cytotoxicity***

The *in vitro* cytotoxicity of the antitubercular active compounds with MIC ≤12.5µg/mL were assessed by 3-(4,5-dimethylthiazol-2-yl)-2,5-diphenyltetrazolium bromide (MTT) assay against growth inhibition of HEK-293 (Human Embryonic Kidney) cells at 50 µg/mL concentration. Cell lines were maintained at 37 °C in a humidified 5% CO_2 incubator (Thermo scientific). Detached the adhered cells and followed by centrifugation to get cell pellet. Fresh media was added to the pellet to make a cell count using haemocytometer and plate 100µL of media with cells ranging from 5,000-6,000 per well in a 96-well plate. The plate was incubated overnight in CO_2 incubator for the cells to adhere and regain its shape. After 24 h cells were treated with the test compounds at 50µg/mL diluted using the media to deduce the percentage inhibition on normal cells. The cells were incubated for 48 h to assay the effect of the test compounds. Zero hour reading was noted down with untreated cells and also control with 1% DMSO to subtract further from the 48 h reading. After 48 h incubation, cells were treated by MTT (4,5-dimethylthiazol-2-yl)-2,5-diphenyltetrazolium bromide) dissolved in PBS (5 mg/mL) and incubated for 3-4 h at 37 °C. The formazan crystals thus formed were dissolved in 100µL of DMSO and the viability was measured at 540 nm on a multimode reader (Spectra max). The values were further calculated for percentage inhibition which in turn helps us to know the cytotoxicity of the test compounds.

4.5. ***Nutrient starvation model***

M. tuberculosis (H37Rv strain) culture (O.D. of 0.8-1.0) grown in Middlebrook 7H9 broth supplemented with OADC (growth supplement) was centrifuged and pellet was washed twice with PBS (Phosphate Buffer Saline, HiMedia) to remove broth completely. Further pellet was re-

suspended in PBS in sealed bottles and incubated at 37 °C for six weeks. During this time bacteria will go into dormant stage followed by inhibitory testing with standard drugs like Ionized (INH), and Moxifloxacin (MOX) along with synthesized compounds for 7 days at a concentration of 10 µg/mL. Next step is to dilute cell suspensions 10-fold up to 10-6 using Middlebrook 7H9 broth with 10% OADC and 100 µl of each dilution was plated in sterile 48 well plates containing 450 ml of Middlebrook 7H9 broth with 10% OADC in triplicates. The plates were kept for incubation at 37 °C for four weeks. Wells with visible bacterial growth were counted as positive, and most probable number (MPN) values were calculated using standard statistical methods [33,34].

4.6. *In vivo activity assay in zebrafish*

Most active compound from *in vitro* assays was taken for testing at *in vivo* level. *M. marinum* strain (ATCC BAA-535) (genetically a close relative of *M. tuberculosis*) incubated at 30 °C in Middlebrook 7H9 broth was infected to adult zebrafish as follows. Fishes were initially weighed and divided accordingly into control and treatment groups (n = 6). All the groups were infected by intraperitoneal route with 20 µl of bacterial culture (around 0.75 million bacterial cells) for a week maintaining fish chamber at 25 °C. After the infection has attained, fishes were administered with test drug orally for a 7 day treatment period with 10 mg/kg dose (for INH 5 mg/kg). Further after treatment period was completed the fishes were sacrificed (fishes were suspended for few minutes in Kanamycin to kill the external bacteria on fishes and to minimize the interference of any other bacteria), the tissue was homogenized and sample was prepared in Middlebrook 7H9 broth. The plates were checked for bacterial count using MPN assay method [35].

4.7. *Molecular docking studies in silico*

In silico analysis were performed in Dell Precision T7610 workstation (8 processors; 8 GB RAM; NVIDIA 3GB graphics; Maestro 9.8, Schrodinger, New York, U.S.A) workstation running on Redhat 6.1 Linux environment. The structure of ligand was drawn in ChemDraw Ultra 6.0. The 3D coordinate file of target protein was retrieved from protein data bank (PDB). Molecular docking studies were performed against *Mycobacterium tuberculosis* enzymes, enoyl reductase (InhA), PDB ID: 4TZK; Decaprenylphosphoryl-β-d-ribose 2'-epimerase (DprE1), PDB ID: 4P8N; Alcohol dehydrogenase (ADH), PDB ID: 2VHW; (3R)-hydroxyacyl-ACP dehydratase (HadAB), PDB ID:4RV2; Lysine-ε aminotransferase (LAT), PDB ID: 2CJD; Topoisomerase (DNA Gyrase),

PDB ID: 5BS8 and Glutamate recemase (MurI), PDB ID: 5H7J. The protein was prepared with the help of Protein Preparation Wizard of Schrödinger Suite 9.8. The prepared protein was optimized and minimized using algorithm OPLS_2005 (optimized potential for liquid simulations) force field and grid was generated using the Glide Grid Generation panel in Glide. The co-crystallized inhibitor 1-cyclohexyl-*N*-(3,5-dichlorophenyl)-5-oxopyrrolidine-3-carboxamide and test compounds were energy minimized using LigPrep module. The minimized test compounds were docked using Glide XP docking calculations. The XP Glide scoring function was used to get the best ranked compounds and the specific interactions like H-bonds, π-cation and π-π stacking and van der Waals were analyzed using XP visualizer in Glide module [36,38].

4.8. *Molecular Dynamics simulations*

The Desmond module from Schrodinger was used for running MD simulations with periodic boundary conditions. Receptor and ligand complex was immersed in an orthorhombic simulation box, with the TIP4P explicit water model using the System Builder Panel with the minimum thickness of a solvent layer, 10 Å. In order to neutralize the system, counter ions were added. Before equilibration and long production of MD simulations, the systems were minimized and pre-equilibrated using relaxation routine implemented in Desmond. Whereas, program ran six steps composed a) energy minimization was used by hybrid method of steepest descent and limited-memory Broyden-Fletcher- Goldfarb-Shanno (LBFGS) algorithm with a maximum steps of 2000 including preliminary 10 steps of steepest descent with solute restrained, b) Energy minimization for 2000 steps without solute restraints, c) 12ps simulation in NVT ensemble (temperature 10K) restraining nonhydrogen solute atoms, d) 12ps simulation in the NPT ensemble (temperature 10K) restraining non-hydrogen solute atoms, e) 24ps simulation in the NPT ensemble restrained along with solute non-hydrogen atoms (temperature 300K) and f) 24ps simulation in the NPT ensemble (temperature 300K) with no restraints respectively. The temperatures and pressures in the short initial simulations were checked by applied Berendsen thermostats and barostats algorithms. The equilibrated system was simulated for 50ns with a time step of 2fs, NPT ensemble was used a Nose-Hoover thermostat at 300K and Martyna-Tobias- Klein barostat at 1.01325 pressure bar. A time step of 1.2fs was used. Saving energy and structure enumerated for every 9.6 ps during simulation, the MD trajectory was generated. Finally to analyze trajectory simulation, a simulation interaction diagram tool was used [39, 40].

4.9 X-ray Crystallography: X-ray data for the compound **4j** was collected at room temperature using a Bruker Smart Apex CCD diffractometer with graphite monochromated MoKα radiation (λ=0.71073Å) with ω-scan method. Preliminary lattice parameters and orientation matrices were obtained from four sets of frames. Integration and scaling of intensity data were accomplished using SAINT program [41]. The structure was solved by direct methods using SHELXS97 and refinement was carried out by full-matrix least-squares technique using SHELXL97 [42]. Anisotropic displacement parameters were included for all non-hydrogen atoms. The N-bound H atom was located in difference Fourier maps, and their positions and isotropic displacement parameters were refined. All other H atoms were located in difference Fourier maps and subsequently geometrically optimized and allowed for as riding atoms, with C-H = 0.93- 0.97 Å, with $U_{iso}(H) = 1.5U_{eq}(C)$ for methyl H or $1.2U_{eq}(C)$. The methyl groups were allowed to rotate but not to tip.

Crystal Data for 4j: $C_{16}H_{19}N_4OS_3Cl$ (M =415.01 g/mol): monoclinic, space group $P2_1/c$ (no. 14), a = 17.1430(6) Å, b = 9.4670(4) Å, c = 12.4260(8) Å, β = 101.909(2)°, V = 1973.24(17) Å^3, Z = 4, T = 294.15 K, μ(Mo Kα) = 0.523 mm^{-1}, $Dcalc$ = 1.3969 g/cm^3, 22404 reflections measured (4.86° ≤ 2Θ ≤ 56.74°), 4755 unique (R_{int} = 0.0180, R_{sigma} = 0.0144) which were used in all calculations. The final R_1 was 0.0489 (I>2σ(I)) and wR_2 was 0.1440 (all data). CCDC 1511250 contains supplementary Crystallographic data for the structure. These data can be obtained free of charge at www.ccdc.cam.ac.uk/conts/retrieving.html [or from the Cambridge Crystallographic Data Centre (CCDC), 12 Union Road, Cambridge CB2 1EZ, UK; fax: +44(0) 1223 336 033; email: deposit@ccdc.cam.ac.uk].

Acknowledgement:

The authors thank Science and Engineering Research Board (SERB), the Department of Science and Technology, the Government of India (EMR/2017/002946) for financial support. SKM is thankful to UGC for senior research fellowship. CSIR- IICT communication no. is IICT/Pubs./ 2019/076.

References:

[1] The Top 10 Causes of Death; World Health Organization: Geneva, 2017. http://www.who.int/mediacentre/factsheets/fs310/en/

[2] World Health Organization (WHO), WHO Global Tuberculosis Report 2018, WHO, Geneve, Switzerland, 2018. http://www.who.int/tb/publications/global_report/en/

[3] M. J. A. Reid, N. Arinaminpathy, A. Bloom, B. R. Bloom, C. Boehme, R. Chaisson, D. P. Chin, G. Churchyard, H. Cox, L. Ditiu, M. Dybul, J. Farrar, A. S. Fauci, E. Fekadu, P. I. Fujiwara, T. B Hallett, C. L. Hanson, M. Harrington, N. Herbert, P. C. Hopewell, C. Ikeda, D. T. Jamison, A. J. Khan, I. Koek, N. Krishnan, A. Motsoaledi, M. Pai, M. C. Raviglione, A. Sharman, P. M. Small, S. Swaminathan, Z. Temesgen, A. Vassall, N. Venkatesan, K. Weezenbeek, G. Yamey, B. D. Agins, S. Alexandru, J. R. Andrews, N.Beyeler, S. Bivol, G. Brigden, A. Cattamanchi, D. Cazabon, V. Crudu, A. Daftary, P. Dewan, L. K. Doepel, R. W. Eisinger, V. Fan, S. Fewer, J. Furin, J.D. Goldhaber-Fiebert, G. B. Gomez, S. M. Graham, D. Gupta, M. Kamene, S. Khaparde, E. W Mailu, E. O. Masini, L. McHugh, E. Mitchell, S. Moon, M. Osberg, T. Pande, L. Prince, K. Rade, R. Rao, M. Remme, J. A. Seddon, C. Selwyn, P. Shete, K. S. Sachdeva, G. Stallworthy, J.F. Vesga, V. Vilc, E. P. Goosby, Lancet. 393 (10178) (2019) 1331-1384.

[4] B. Ki-Moon, Lancet., 393 (10178) (2019) 1268-1270.

[5] R. Ansumana, S. Keitell, G. M. Roberts, F. Ntoumi, E. Petersen, G. Ippolito, A. Zumla, Int. J. Infect. Dis. 56 (2017) 101.

[6] S. Baghdadi. Int. J. Mycobacteriol. 5 (2016) S14.

[7] K. Dheda, C. E. Barry, G. Maartens, Lancet. 387 (10024) (2016) 1211-1226.

[8] G. B. Migliori, G. De Iaco, G. Besozzi, R. Centis, D. M. Cirillo, Euro Surveill. 12 (5) (2007) E070517.1

[9] J. A. Caminero, G. Sotgiu, A. Zumla, G. B. Migliori, Lancet. Infect. Dis.10 (9) (2010) 621-629.

[10] K. Duncan, Tuberculosis. 83 (1-3) (2003) 201-207.

[11] L. Guglielmetti, M. Jaspard, D. Le Dû, M. Lachâtre, D. Marigot-Outtandy, C. Bernard, , N. Veziris, J. Robert, Y. Yazdanpanah, E. Caumes, M. Fréchet-Jachym, French MDR-TB Management Group. Eur. Respir. J. 49 (2017) 1601799.

[12] G. J. Fox, D. Menzies, Infect. Dis. Ther. 2 (2) (2013) 123-144.

[13] G. Sotgiu, E. Pontali, R. Centis, L. D Ambrosio, G. B. Migliori, Anti-Infect. Ther. 13 (3) (2015) 305-315.

[14] L. E. Bermudez, P. Kolonoski, L. E. Seitz, M. Petrofsky, R. Reynolds, M. Wu, L. S. Young. Antimicrob. Agents. Chemother. 48 (9) (2004) 3556-3558.

[15] F. M. Shahab, F. Kobarfard, B. Shafaghi, S. Dadashzadeh, Xenobiotica. 40 (3) (2010) 225-234.

[16] A. E. Grzegorzewicz, N. Eynard, A. Quémard, E. J. North, A. Margolis, J. J. Lindenberger, V. Jones, J. Korduláková, P. J. Brennan, R. E. Lee, D. R. Ronning, M. R. McNeil, M. Jackson, ACS Infectious Diseases *1* (2) (2015) 91-97. DOI: 10.1021/id500032q.

[17] A.E. Grzegorzewicz, J. Korduláková, V. Jones, S.E. Born, J.M. Belardinelli, A. Vaquié, V.A. Gundi, J. Madacki, N. Slama, F. Laval, J. Vaubourgeix, R.M. Crew, B. Gicquel, M. Daffé, H.R. Morbidoni, P.J. Brennan, A. Quémard, M.R. McNeil, M. Jackson, J. Biol. Chem. (287) (2012), 38434– 38441. DOI: 10.1074/jbc.M112.400994.

[18] S. Kantevari, S. R. Patpi, D. Addla, S. R. Putapatri, B. Sridhar, P. Yogeeswari, D. Sriram, ACS. Comb. Sci. 13 (2011) 427-435.

[19] S. Kantevari, S. R. Patpi, B. Sridhar, P. Yogeeswari, D. Sriram, Bioorg. Med. Chem. Lett. 21 (4) (2011) 1214-1217.

[20] S. R. Patpi, L. Pulipati, P. Yogeeswari, D. Sriram, N. Jain, B. Sridhar, R. Murthy, T. Anjana Devi, S. V. Kalivendi, S. Kantevari, J. Med. Chem. 55 (8) (2012) 3911-3922.

[21] G. Surineni, S. K. Marvadi, P. Yogeeswari, D. Sriram, S. Kantevari, Bioorg. Med. Chem. Lett. 28 (2018) 1610-1014.

[22] G. Surineni, P. Yogeeswari, D. Sriram, S. Kantevari, Bioorg. Med. Chem. Lett. 25 (2015) 485-491.

[23] S. Kantevari, T. Yempala, G. Surineni, B. Sridhar, P. Yogeeswari, D. Sriram, Eur. J. Med. Chem. 46 (2011) 4827-4833.

[24] A. Jallapally, D. Addla, P. Yogeeswari, D. Sriram, S. Kantevari, Bioorg. Med. Chem. Lett. 24 (2014) 5520-5524.

[25] L. Pulipati, J. P. Sridevi, P. Yogeeswari, D. Sriram, S. Kantevari, Bioorg. Med. Chem. Lett. 26 (2016) 3135-3140.

[26] G. Surineni, P. Yogeeswari, D. Sriram, S. Kantevari, Med. Chem. Res. 24 (3) (2015) 1298-1309.

[27] L. Pulipati, P. Yogeeswari, D. Sriram, S. Kantevari, Bioorg. Med. Chem. Lett. 26 (2016) 2649-2654.

[28] S. Kantevari, S. R. Patpi, D. Adala, B. Sridhar, Synthesis. (2010), 3745-3754.

[29] L. A. Collins, S. G. Franzblau, Antimicrob. Agents Chemother. 41 (5) (1997) 1004-1009.

[30] S. K. Marvadi, V. S. Krishna, D. Sriram, S. Kantevari, Eur. J. Med. Chem. 164 (2019) 171-178.

[31] D. S. Agarwal, V. S. Krishna, D. Sriram, P. Yogeeswari, R. Sakhuja, Steroids. 139 (2018) 35-44.

[32] S. K. Marvadi, V. S. Krishna, D. Sriram, S. Kantevari, Bioorg. Med. Chem. Lett. 29 (4) (2019) 529-533.

[33] J. C. Betts, P. T. Lukey, L. C. Robb, R. A. McAdam, K. Duncan, Mol. Microbiol. 43 (2002) 717-731.

[34] V. S. Krishna, S. Zheng, E. M. Rekha, L. W. Guddat, D. Sriram, J. Comp. Aid. Mol. Des. 33 (3) (2019) 357-366

[35] J. P Sridevi, H. S. Anantaraju, P. Kulkarni, P. Yogeeswari, D. Sriram. Int. J. Mycobacteriol. 3 (4) (2014) 259-267.

[36] X. He, A. Alian, R. Stroud, P.R. Ortiz de Montellano, J. Med. Chem. 49 (21) (2006) 6308-6323.

[37] M. Daffé, A. Quémard, H. Marrakchi, Mycolic Acids: From Chemistry to Biology, Geiger O. (eds) Biogenesis of Fatty Acids, Lipids and Membranes. *Handbook of Hydrocarbon and Lipid Microbiology*. Springer, Cham, (2017)**,** 1-36. DOI: 10.1007/978-3-319-43676-0_18-1

[38] G. Kumar, V. S. Krishna, D. Sriram, S. M. Jachak, Eur. J. Med. Chem. 156 (2018) 871-884.

[39] P. D. Lyne, M. L. Lamb, J. C Saeh, J. Med. Chem. 49 (2006) 4805-4808.

[40] G. J. Martyna, D. J. Tobias, M. L. Klein, J. Chem. Phys. 101 (1994) 4177-4189.

[41] Bruker. SAINT, Version 6.28a, and SMART, Version 5.625, Bruker AXS Inc. Madison, WI, 2001.

[42] G. M. Sheldrick, Acta Crystallogr A. 64 (2008) 112-122.

Graphical Abstract

Synthesis, *in vitro* and *in vivo* (Zebra fish) antitubercular activity of 7,8-dihydroquinolin-5(6*H*)-ylidenehydrazinecarbothioamides

Sandeep kumar Marvadi, Vagolu Siva Krishna, Goverdhan Surineni, Rudraraju Srilakshmi Reshma, Balasubramanian Sridhar, Dharmarajan Sriram, Srinivas Kantevari,

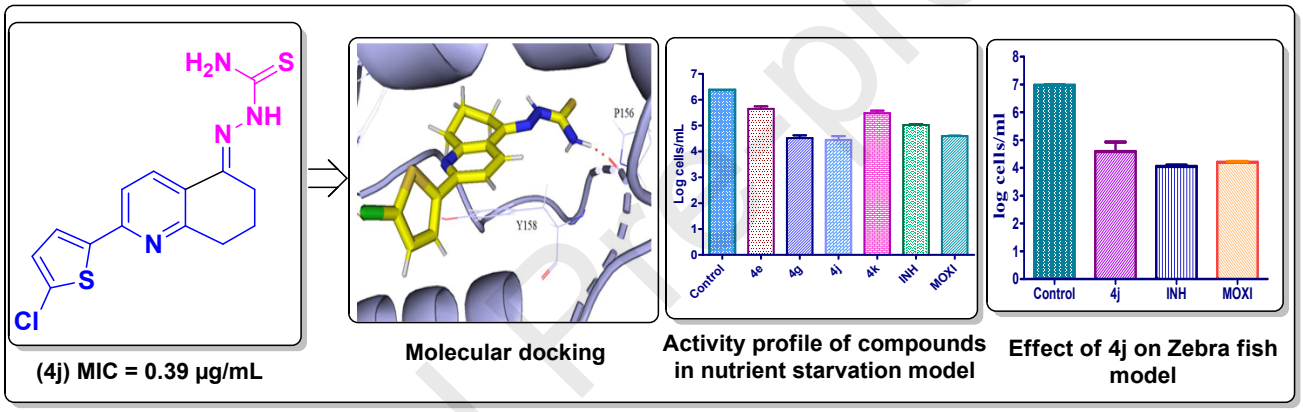

Highlights

1. Twenty-two new 7,8-dihydroquinolin-5(6*H*)-ylidenehydrazinecarbothioamides **4a–v** was synthesized.
2. Compounds **4e** & **4j (**MIC 0.39 μg/mL) & **4a, 4g** and **4k** (MIC 0.78 μg/mL) were found to inhibit *Mycobacterium tuberculosis (Mtb)*H37Rv.
3. Hydrazinecarbothioamide derivatives **4a-k** exhibited enhanced activity than **3a-k** even if the other framework and substituents are same.
4. The *in vivo (Zebra fish)* antimycobacterial screening led to the identification of hit compound **4j**.
5. **4j** exhibited significant activity in *Mtb* nutrient starvation model (2.2-fold reduction).

Declaration of interests

- ✓ **The authors declare that they have no known competing financial interests or personal relationships that could have appeared to influence the work reported in this paper.**

☐The authors declare the following financial interests/personal relationships which may be considered as potential competing interests: